Evaporation of process water from recycled containerboard mills

STEFAN BÜRGMAYR, JOANNE TANNER, WARREN BATCHELOR, AND ANDREW A.F. HOADLEY

ABSTRACT: The reduction of the specific effluent discharge volumes of paper mills leads to concentrated process waters that are difficult to treat. Evaporation is an effective water reclamation technology; however, its feasibility largely depends on the fouling behavior of the calcium rich process water.

A pilot plant study was conducted to investigate fouling of an evaporator processing the production water from a recycled containerboard mill. The evaporator was operated continuously for five weeks at an evaporation temperature of 55°C and a differential temperature of 5°C, and with a recovery rate of approximately 90%. The calcium ion concentration of the circulating liquor exceeded 7,000 mg/L with a pH of 6.

Despite the high fouling potential of the circulating liquor, the heat transfer coefficient did not decline over the investigated trial. The absence of deposits on large areas of the heating surfaces demonstrate that the process water does not generally form deposits under the conditions that were investigated. Calcium sulfate deposits were only found in areas where there was inadequate coverage of liquid over the heating surfaces.

The findings show that evaporators can be used to effectively close the water system of recycled containerboard mills without fouling impacting the energy efficiency.

Application: This work demonstrates for the first time, in a long-duration pilot plant study, the successful use of evaporation to reclaim water from the process water of a recycle containerboard mill without negative impact on its energy balance. For this purpose, a custom-built low-temperature vacuum evaporator pilot plant was installed on-site at a paper mill to investigate operation, selective separation efficiency, and feasibility under relevant conditions.

In 2017, around 422 million metric tons of paper and paperboard were manufactured worldwide [1]. Of this, the largest paper segment was recycled containerboard with 33% [2]. The average specific effluent discharge volume of European recycled paper mills is approximately 5.5 m³/metric ton [3]. This data suggests a theoretical wastewater discharge volume of 776 million m³ from recycled containerboard mills every year. The industry's global impact on water resources increases with its annual growth rate, which was 2.7% in 2017 [4]. Water scarcity and related challenges require commercial water consumers to respond by implementing strategies for water stewardship and best practice [5]. This has led to renewed interest in zero liquid discharge schemes using thermal separation processes [6].

Water system closure in the paper industry

Zero liquid discharge or water system closure has been a long-standing goal for the water intensive paper industry. Since the 1970s, the specific effluent discharge volume of paper and board mills has been successively reduced from close to 50 m³/metric ton to less than 10 m³/metric ton; however, since 2000, no significant reductions were realized [7]. Recycled containerboard mills operate with the lowest specific water discharge volumes of all paper grades. Recycled packaging paper mills in Germany, for example, were found to operate with a specific effluent discharge volume of 3 m³/metric ton on average [8]. Completely closed water systems are rare, because system closure is accompanied by an exponential accumulation of non-fibrous materials in the process water that adversely affects production and product quality [9]. In recycled containerboard mills, these substances are primarily starch and calcium carbonate that enter the production process with the recovered paper. Up to 65 kg of starch in the form of strength agent and water-based glue enters the process with each metric ton of recycled packaging paper grades [10]. Up to 38 kg of calcium carbonate in the form of filler and coatings are introduced with every metric ton of recycled graphical paper grades [11]. It was found that 50%–70% of the starch is released into the water during repulping [12]. Starch dissolves in the process water and hydrolyzes to glucose, which provides the nutritional basis for anaerobic bacteria. Anaerobic fermentation converts glucose into volatile fatty acids (VFAs), which again dissolve calcium carbonate [13]. Moreover, the content of kraft fibers (sulfate pulping) contained in the recycled packaging grades introduces sodium and sulfate ions into the process, which are derived from sodium sulfate that is used in kraft pulping to produce fiber pulp. As completely closed systems are rare, little data is published on the process water parameters of such systems. **Table I** shows industrial data published in the literature for three recycled containerboard mills with completely closed water systems. The previous theory and the examples shown in Table I indicate that the process water of recycled containerboard mills can be characterized by high organic substances such as VFAs, as well as calcium ion concentrations.

The high chemical oxygen demand (COD) concentra-

	Unit	Smurfit Kappa Zülpich [14]	Mill A [15]	Mill B [15]
Specific discharge volume	m^3/metric ton	0	0	0.3
Ca^{2+}	mg/L	2,650	2,100	2,000
pH	-	6.3	6.6	6.4
VFAs*	mg/L	7,250	-	-
COD	O_2mg/L	32,800	40,000	-
SO_4	mg/L	1,350	1,800	1,500
Temperature	°C	-	51	38
TOC	mg/L	-	-	10,300

* Sum of acetic, propionic and n-butyric acid.
Ca^{2+} = calcium ion; VFAs = volatile fatty acids; COD = chemical oxygen demand, SO_4 = sulfate; TOC = total organic carbon.

I. Process water parameters of three recycled containerboard mills with closed water systems.

tions of 32,800 and 40,000 O_2mg/L, as well as the high total organic carbon (TOC) of 10,300 mg/L, of the process waters shown in Table I are indicators for high concentrations of dissolved organic substances, such as starch and its degradation products, in the water. The presence of VFAs with a concentration of more than 7,000 mg/L is evidence for ongoing anaerobic fermentation in the process [13]. The calcium ion concentration of 2,000 to 2,650 mg/L indicates calcium carbonate dissolution due to the presence of VFAs. Prior research studied the impact of water system closure in recycled containerboard mills on process water characteristics and calcium carbonate solubility in order to evaluate the suitability of water treatment technologies [16].

Commonly used technologies to treat the process water of recycled containerboard mills are biological treatment and membrane filtration. Biological water treatment in paper mills was established in the 1980s and is mostly designed as combined anaerobic/aerobic stages [17]. In the anaerobic reactor, the dissolved organic substances are converted into biogas [18]. To facilitate this methagonesis, the pH needs to be near neutral. This and the fact that the biogas contains approximately 20% carbon dioxide leads to the reformation of calcium carbonate [18]. Calcification of anaerobic sludge granules and deposition of precipitate in the reactor adversely affect the degradation efficiency and cause operational problems. This is a widespread problem for paper mills operating with concentrated process waters due to advanced water system closure [19-21]. Membrane filtration such as ultrafiltration, nanofiltration, and reverse osmosis can be used to remove dissolved organic and inorganic substances down to monovalent ions from process water [22]. However, the main issue is fouling of the membrane pores due to deposition of contaminants [23]. The combination of biological treatment and membrane filtration, to first reduce the organic content and subsequently remove the inorganic constituents, was found to be unsuccessful in pilot scale because of fouling [24]. The same conclusion was drawn from a full-scale implementation in industry that was abandoned after two years of optimization [25]. These negative experiences suggest that biological treatment as well as membrane filtration are too sensitive to treat the highly concentrated process water from recycled containerboard mills with restricted water systems.

Evaporation

The principle of evaporation is based on thermal separation of a solvent from a solution due to differences in boiling points. In contrast to biological treatment, evaporation does not introduce carbonates that would cause calcium carbonate formation. It further does not have the risk of plugging, because it does not use a filter medium. Laboratory trials demonstrated that evaporation efficiently removes nonvolatile inorganic contaminants from the white water of a thermomechanical pulp mill [26]. Another study also found a high removal efficiency for organic substances [27]. Therefore, evaporation is capable of producing a condensate suitable to substitute freshwater from process water that is difficult to treat with conventional methods, thereby potentially eliminating effluent and achieving complete water system closure.

Evaporators in the pulp and paper industry find application in chemical pulp mills that are based on the sulfate process. Cellulose fibers are extracted from wood chips by cooking them in a strong alkaline solution of sodium hydroxide and sodium sulfide [28]. The solution with extracted lignin is then concentrated in evaporators from 15%–20% to 70%–80% dry solids content, which makes it possible to incinerate the liquor to recover pulping chemicals and generate energy [29]. In the early 1990s, two Canadian mechanical pulp mills started using evaporators to eliminate liquid waste from their production processes [30,31]. More mills followed the example in other parts of the world

[32,33]. In this process, the diluted process water with a dry solids content of approximately 2% is first concentrated using mechanical vapor recompression evaporators until it reaches a solids content of 35%. Subsequently, steam driven multiple effect evaporators further increase the solids content to 70%, which allows incineration of the concentrate [34]. In recycled containerboard mills, wastewater evaporators are rare, though examples do exist. An evaporator with polymeric heat exchange surfaces was installed at a mill in Saudi Arabia for the treatment of saline groundwater and process water. The concentrate is disposed of at a liquid waste dump [35]. A mill in the desert of New Mexico uses an evaporative crystallizer to treat the concentrate from upstream membrane filtration [36]. In Mexico, a mill uses four multiple-effect evaporators and an evaporative crystallizer to achieve zero liquid discharge [37].

The limited use of evaporators in recycled containerboard mills is in part due to the high investment and operational cost. High investment costs for evaporators are due to the large heating surfaces made from corrosion-resistant metal and potentially expensive surface finish. The specific energy consumption of effluent evaporators in mechanical pulp mills is reported to be between 17 and around 20 kWh/m³ (or 72 kJ/kg) [33,34,38]. The previously-mentioned evaporator with polymeric heating surfaces has a specific energy consumption of 9–13 kWh/m³ (or 32–47 kJ/kg) [39]. This is due to the low evaporation temperature of 50°C–65°C and a very small differential temperature of less than 2.5°C [40,41]. The practicality of implementing evaporators in recycled containerboard mills depends not only on investment and energy costs but also on the deposition of substances on heat exchange surfaces, which can decrease energy efficiency and require extra cleaning and maintenance efforts.

Fouling

Fouling describes unwanted deposit formation on heat exchange surfaces [42]. The insulating effect of the additional foulant layer increases the thermal resistance and reduces the overall energy efficiency of heat exchange equipment. Fouling can become a chronic operational problem. A survey in New Zealand found that approximately 90% of the investigated heat exchangers experience fouling [43]. Fouling is accompanied by significant operational and economic consequences, such as production loss and reduced runtimes between cleaning intervals, as well as related safety and environmental hazards [43]. In anticipation of fouling, additional cleaning equipment becomes necessary and heat exchange surfaces are deliberately oversized by design [44]. The total cost for heat exchanger fouling was estimated to be 0.28% to 0.35% of the gross national product (GNP) in the USA [45] and 0.2% to 0.33% of the GNP in the UK [46, 47].

Due to the high calcium ion concentration in the process water of recycled containerboard mills, as shown in Table I, this study focuses on precipitation fouling caused by the crystallization of the calcium salts, namely, calcium carbonate ($CaCO_3$) and calcium sulfate ($CaSO_4$). The thermal conductivities of $CaCO_3$ and $CaSO_4$ are 2.9 and 2.3 W/m*K, respectively, compared to 16 W/m*K for stainless steel [48]. These low values mean that the presence of even a thin layer of calcium salts will dominate the overall heat transfer resistance, especially considering the thin stainless-steel sheet thickness of most heat exchanger surfaces of approximately 12 mm.

The mechanism of precipitation fouling consists of three steps. First, the aqueous salt solution supersaturates. Then, a nucleus is formed, which consequently acts as a seedling for crystal growth on the heat exchanger surface [49]. This process is governed by simultaneous deposition and erosion of the foulant from the heating surface [50]. Numerous factors influence the deposition rate, including fluid properties, heat exchange surface characteristics, and operating conditions [51].

The fluid properties determine the dissolved solids saturation and subsequent formation of precipitated particles that can attach to surfaces in the first place. As the fouling mechanism is initiated by forming a nucleus, the supersaturation of dissolved salts in the fluid is considered the most important factor influencing the rate of fouling [52]. It was found that with increasing concentration of ions, the formation of a nucleus, as well as the deposition rate of $CaCO_3$, increases [53]. The pH is also important for $CaCO_3$ deposition, as it influences the presence of counter ions by shifting the carbonic acid–carbonate equilibrium [54].

Surface properties of the evaporator heat exchange surfaces, such as roughness and topography, influence the initial deposition, as they affect the particle adhesion. Smooth surfaces offer less nucleation sites [55]. Roughness provides more surface area and consequently increases the chance for deposition [56]. For example, the attraction of particles in a synthetic sea water solution to a 90–10 copper-nickel surface with a roughness, *Ra*, of 1.27 µm (standard mill finish) was several times higher than to a mirror finish surface with *Ra* of 0.127 µm [57]. It was also shown that the weight of the deposit of crystallization fouling of calcium carbonate on stainless-steel plates increased with surface roughness and topography [58]. Low surface free energy is related to less attachment and easier cleaning. However, there is no simple, direct correlation between surface free energy itself and fouling, as the molecular interactions also depend on smoothness of the surface and the crystalline properties of the deposit [59].

Evaporator operating conditions such as hydrodynamics and thermal conditions further influence fouling. One paper found that crystal growth increases with surface temperature and decreases with increasing flow velocity [60]. The fouling rate increases with higher surface temperature [61,62], higher differential temperature [61,63], and lower flow rate [61,64,65]. Research showed that the wetting area

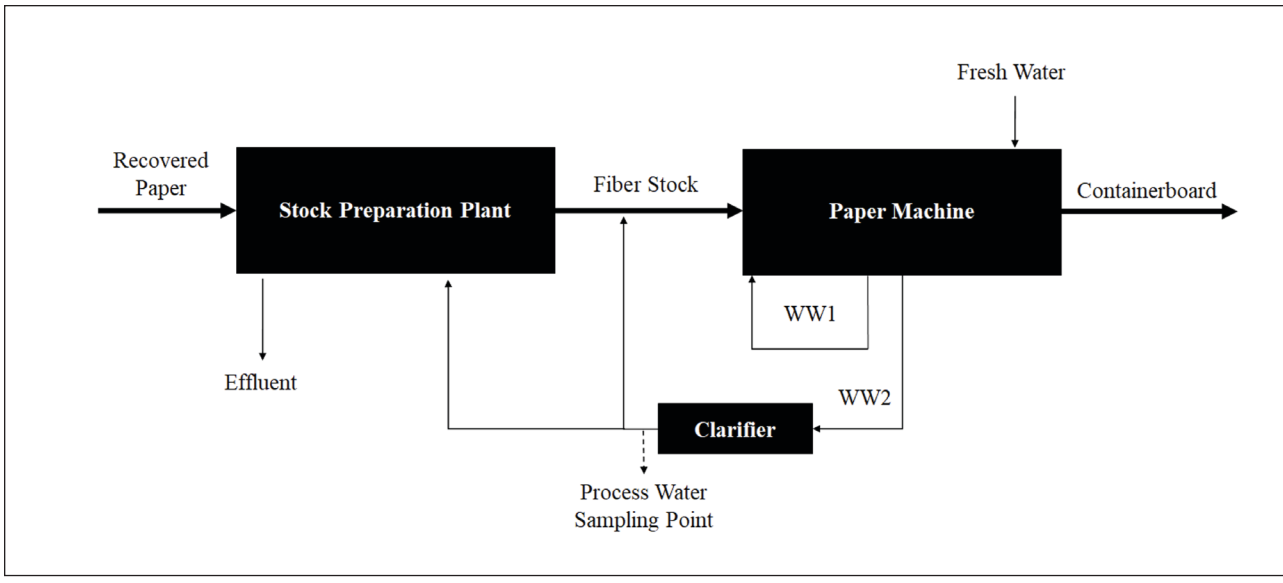

1. Simplified illustration of the water system of a recycled containerboard mill with internal water clarification (WW = white water).

of a falling film is reduced at low temperatures and flow rates due to film shrinkage, especially at the bottom of the heating surface [66].

The heat transfer capacity of fouled evaporators may be recovered by periodic cleaning. A mill survey found that black liquor evaporators were cleaned three times per month on average, with some evaporators requiring up to twelve cleaning shutdowns per month [67]. A study on black liquor evaporation concluded that deposit formation can be reduced by reducing evaporation temperature and differential temperature. Furthermore, deposit formation increased with higher solids content. The deposits were identified as water soluble and fibrous [68]. A laboratory study found that the deposits in an evaporator for effluent treatment from a mechanical pulp mill were mostly organic matter. The heat transfer coefficient (HTC) was reduced by more than 30% after only 40 h of operation [69]. In one investigation, an effluent evaporator in a mechanical pulp mill required pressure cleaning on a monthly cycle, which took the evaporator unit off process for 24 h [33].

Crystallization fouling of $CaCO_3$ is primarily mitigated by reducing the pH to transform carbonate species into carbonic acid/dissolved carbon dioxide. Calcium sulfate is not pH dependent; deposit formation of $CaSO_4$ was shown to be mitigated successfully by the addition of 0.1 g/L of ethylenediaminetetraacetic acid (EDTA) [70]. Cleaning $CaSO_4$ deposits was found to be effectively done by using a sodium carbonate (Na_2CO_3) solution at elevated temperature [71].

In summary, water system closure in recycled containerboard mills has reached a technical limit due to the build-up of dissolved substances in the process water. The high contaminant concentrations in the process water make it difficult to purify the water with conventional technologies. Evaporation may be a suitable and effective solution. However, heat exchange surface fouling can significantly reduce its feasibility. There is virtually no information publicly available on the fouling potential of process water from recycled containerboard mills in evaporators. This research studies the fouling behavior of process water from recycled containerboard mills in a custom-built pilot scale vacuum evaporator. It includes the impact of deposits on heat transfer, deposit characterization, and cleaning strategies.

MATERIALS AND METHODS

Process water

The trial was conducted with clarified process water from an Australian recycled containerboard mill. The mill recycles old corrugated containerboard (OCC) with a content of up to 30% mixed recovered paper grades as raw material for the annual production of 140,000 metric tons of linerboard and corrugated medium. The water system of the paper mill is restricted and discharges on average 2.4 m^3 of effluent per metric ton of paper produced. **Figure 1** shows a schematic of the containerboard recycling process, water system, and process water sampling point.

Water analytics

pH

The measurement was performed in accordance with APHA Method 4500-H+B "pH Value in water by potentiometry using a standard hydrogen electrode." In the laboratory, a Metrohm 855 robotic titrosampler (Metrohm; Herisau, Switzerland) was used.

Total suspended solids (TSS)

The measurement was performed in accordance with APHA method 2540 D&E "Total Suspended solids dried at 103-105°." The TSS are solids that are retained by a glass fiber filter with 2 µm pores (Filtech grade 393). The residue

on the filter is dried in an oven for 2 h at 105°C and weighted afterwards.

Total dissolved solids (TDS, TDS_{org}, TDS_{inorg})

The measurement was performed in accordance with APHA method 2540 C "Total dissolved solids dried at 180°C." The TDS is the portion of solids that passes through a glass fiber filter with 2 µm pores (Filtech grade 393). The water of the filtrate is evaporated and the residue is dried in an oven for 2 h at 105°C. Afterwards, filter and residue are weighed and the mass of non-filterable dissolved solids is calculated.

The organic, as well as inorganic, fractions are determined by combustion in a furnace at 550°C. The organic fraction (TDS_{org}) is determined by the loss on ignition. The incombustible residue of the sample is the inorganic fraction (TDS_{inorg}).

Sulfate

The measurement was performed in accordance with USEPA Method 375.4 "Sulfate by turbidity."

A 5.0 mL conditioning reagent (hydrochloric acid [HCl]; alcohol; sodium chloride [NaCl] solution) was mixed into a 100 mL sample. While stirring, a spoonful of barium chloride ($BaCl_2$) crystals was added and stirred for 60 s. The fluid was transferred into the absorbance cell of a nephelometer, and turbidity was measured every 30 s within 4 min. The maximum reading was recorded and the sulfate concentration was determined in comparison with a sulfate standard curve.

Volatile organic substances

A gas chromatography mass spectrometer with solid phase micro extraction (GC MS SPME) was used to identify the organic volatile substances of the liquid samples.

Five grams of water samples were weighed in 10 mL headspace vials. The vials were sealed with a polytetrafluoroethylene (PTFE) lined septa and heated to 55°C for 20 min. A solid phase micro extraction (SPME) fiber was used to absorb the volatiles from the headspace of the vial. The fiber was then desorbed in the inlet of the gas chromatograph (Agilent 7890A; Agilent Technologies, Santa Clara, CA, USA), and the volatiles were detected and identified by the mass selective detector (Agilent 5975 Series). A chemical ionization spectrum was created and substances that are a 90% or higher match to the criteria of the mass spectrometry library from the National Institute of Standards and Technology (NIST) were identified [72].

Calcium-ion concentration

The calcium ion concentration was measured using an inductively coupled plasma – optical emission spectrometer (ICP-OES). The method was adapted from USEPA Method 2007 "Determination of metals and trace elements in water and wastes by inductively coupled plasma-atomic emission spectrometry." The inductively coupled plasma emission spectrometer (Agilent 720) generates a plasma that energizes atoms in the water sample. When the atoms return to a lower energy level, they emit rays. Depending on emitted wavelength and intensity, atoms are identified and their concentration is quantified.

Evaporator pilot plant

The purpose of the custom-built pilot scale evaporator is to simulate the working principle of a full-scale vacuum evaporator operating with mechanical vapor recompression. The plant consists of three sections: heating, concentration, and separation, as well as a cooling section. The heating section consists of an electric boiler, three heating bodies, and a steam condensate recirculation pump. The electrical boiler generates steam with a temperature of 140°C. The temperatures of the condensing steam (60°C) and the evaporation temperature (55°C) are controlled with venturi fittings that set the required under pressure.

The concentration and separation section consists of the evaporator vessel, a circulation pump, and the distribution system. The circulating concentrate is distributed via 18 flat spray nozzles that create a falling film that flows downwards over six heat transfer surfaces. Water and volatile substances vaporize and exit the evaporator vessel into a condenser that is supplied with cooling water (11°C) to condense the vapor. The concentrate is collected on the bottom of the evaporator vessel and circulated back to the distribution system. A defined volume of concentrate is continuously discharged.

A control panel provides continuous monitoring of temperatures, pressures, and pump operation. From the pump runtimes, in combination with the dimensions and operating conditions of the pilot plant, the evaporation rate and the concentrate discharge flow rate can be calculated. **Figure 2** shows the process and instrumentation diagram, as well as the evaporator pilot plant equipment as installed on site.

The process water is collected from the drum clarifier of a recycled containerboard mill (Fig. 1) and stored in an intermediate bulk container (IBC) tank (~1,200 L) that is refilled once a day. The feed flow rate into the pilot plant is monitored by a magnetic inductive flow meter (IFM, SM7000).

The heat transfer surfaces are vertical lamellas with a sheet thickness of 1.2 mm and cavity width of 6 mm. Two of the installed lamellas are made from austenitic stainless steel (304SS) with a 320 grit surface finish (*Ra* 0.3 µm). The third lamella is made from duplex stainless steel (2205) with a mirror polished surface (*Ra* 0.2 µm). The combined heat transfer area of the three lamellas is 1.0416 m^2. The specific evaporation capacity of the pilot plant is 14.5 kg/($h.m^2$). The recirculation pump has a design flowrate of 1,000 kg/h, resulting in a transfer rate of 960 kg/($h.m^2$). With a combined heating surface width of 1.2 m, the wet-

a)

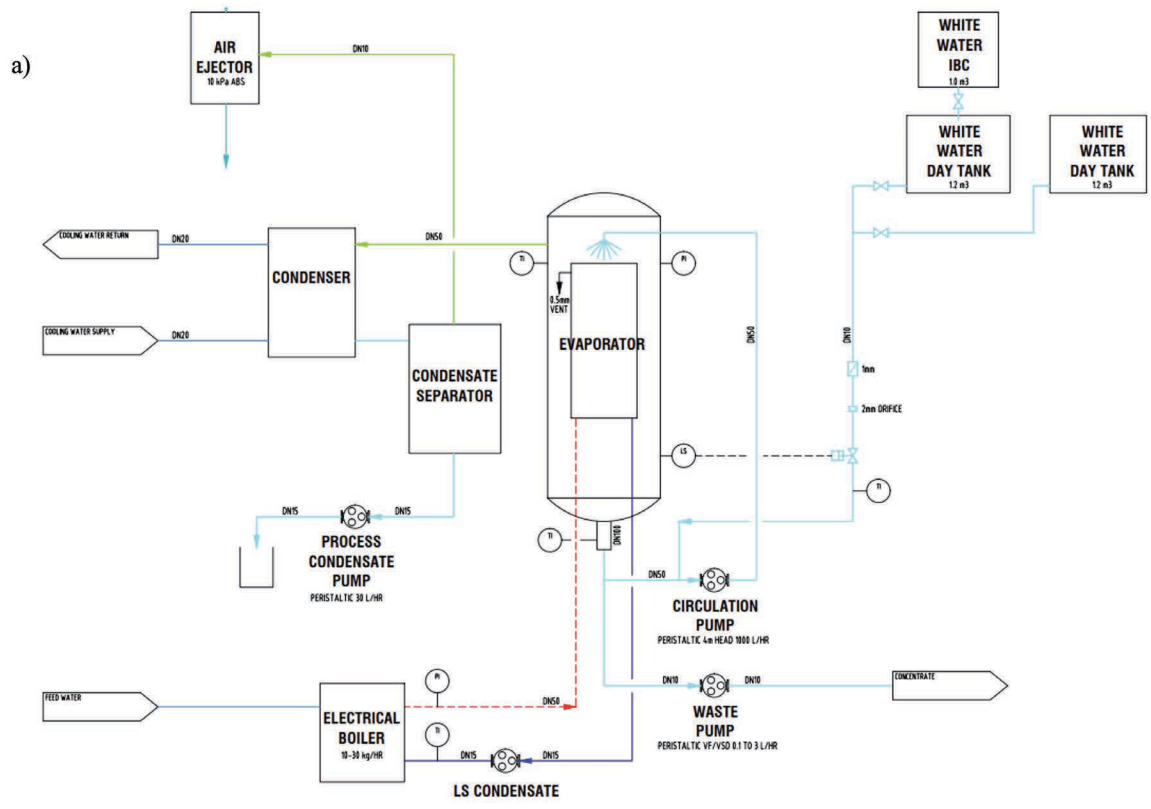

b)

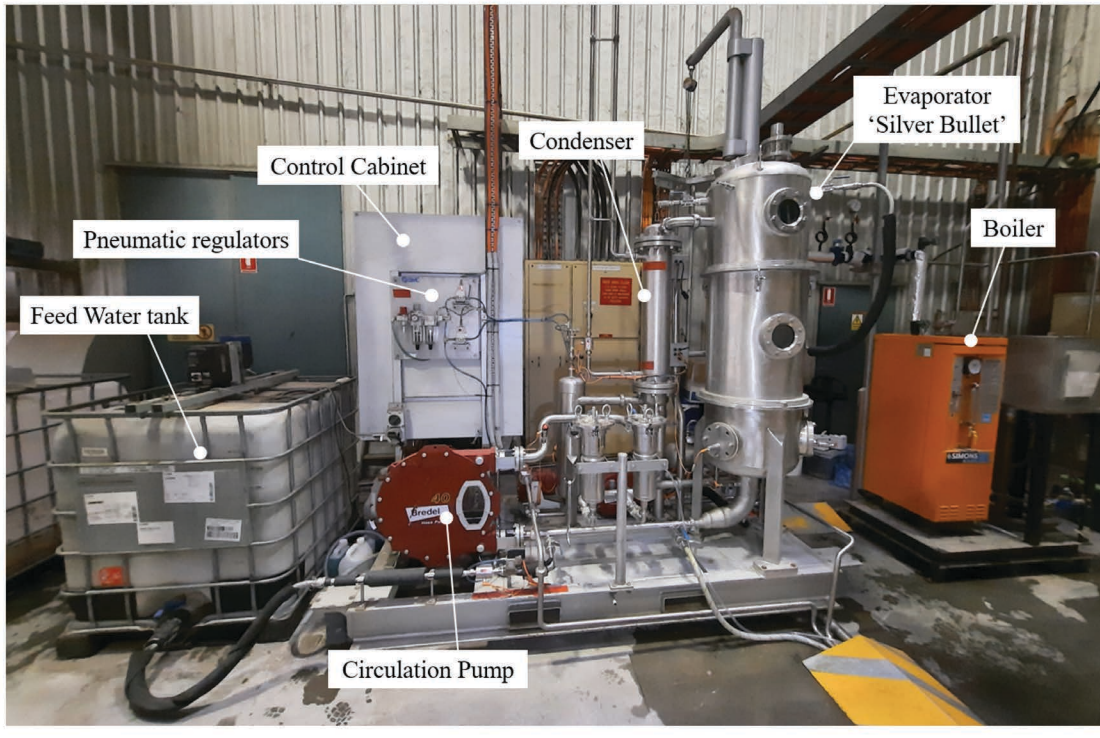

2. Evaporator pilot plant process and instrumentation diagram: (a) process and instrumentation diagram (IBC = intermediate bulk container), and (b) equipment as installed on site.

ting rate can be calculated as 8.9 L/(cm.h).

Preliminary testing confirmed that the liquid distribution system gave an equal flow to each nozzle. The temperature distribution over the heating surfaces is uniform.

Mass balance

The mass balance determines the flow rate of the individual partial streams, the recovery rate, and the concentrating factor.

The feed water flow rate is measured and compared to changes in the level of the feed tank. Condensate as well as concentrate flow rates are calculated from the pump runtime and the displacement volume of the pumps.

$$m_{Feed} = m_{Condensate} + m_{Concentrate} \quad (1)$$

The mass balance (on a volume basis) is within a tolerance of 0.05 L/h. Variations were due to changing displacements volumes of the pumps with ambient temperature.

The ratio of condensate to feed gives the condensate recovery rate (*RR*):

$$RR = \frac{m_{Condensate}}{m_{Feed}} * 100\% \quad (2)$$

The ratio of feed to concentrate gives the volumetric concentration factor (*VCF*):

$$VCF = \frac{m_{Feed}}{m_{Concentrate}} \quad (3)$$

With increasing recovery rate, the concentrating factor increases exponentially. For better control of the pilot plant process, to minimize strong fluctuations, and to obtain reliable data, the concentrating factor was set to around 10.

Considering concentrations of contaminants in the process water as determined from laboratory results, the selectivity of the process and volatility of substances was determined by either removal efficiency of contaminants from the feed water, or concentrating factor of contaminants in the concentrate:

$$c_{Feed} * m_{Feed} = c_{Condensate} * m_{Condensate} + c_{Concentrate} * m_{Concentrate} \quad (4)$$

The specific concentration factor (*CF*) of individual nonvolatile contaminants is the ratio of the concentration of a particular species in the concentrate to the concentration of the same species in the feed water:

$$CF = \frac{c_{Concentrate}}{c_{Feed}} \quad (5)$$

The removal efficiency (*RE*) is the ratio of the concentration of a particular contaminant species in the feed water to the concentration of the same species in the condensate:

$$RE = \frac{cFeed - cCondensate}{cFeed} * 100\% \quad (6)$$

Thermal energy balance

To evaluate the impact of fouling on heat exchange, heat transfer coefficient is monitored. The overall heat transfer coefficient (*U*) is calculated from the heat transfer rate (*Q*), the differential temperature (ΔT), and the heat exchange surface area (*A*):

$$U = \frac{Q}{A * \Delta T} \quad (7)$$

Below is the detailed heat transfer coefficient (*HTC*) calculation based on parameters from the pilot plant control panel:

$$HTC = \frac{[(T_{steam} - T_{condensing}) * C_{p,v} + \Delta H_{vl} + (T_{condensing} - T_{condensate}) * C_{p,l}] * \dot{m}_{steam}}{A * (T_{condensing} - T_{evaporatng})} \quad (8)$$

where $T_{evaporating}$ is the evaporation temperature, T_{steam} is the steam temperature provided by the steam generator, $T_{condensing}$ is the steam condensing temperature, $T_{condensate}$ is the steam condensate temperature, ΔH_{vl} is the latent heat of evaporation of the steam, and $C_{p,v}$ and $C_{p,l}$ are the vapor and liquid specific heat capacities, respectively.

Thickness measurement

The thickness of deposits on the heating surfaces was determined using a coating thickness gauge (VDIAGTOOL VC-100; Shenzhen Chuang Xin Hong Technology Co. Ltd.; Shenzhen, Guangdong, China). The measurement range is 0.0–2.0 mm with a resolution of 0.05 mm. To assure accurate measurements, the deposits were dried for 12 h before using the thickness gauge.

Scanning electron microscopy and energy-dispersive X-ray analysis

An FEI Nova NanoSEM 450 FEG (FEI Co.; Hillsboro, OR, USA) scanning electron microscope (SEM) with an energy-dispersive X-ray (EDX) detector (Quantax 400, Bruker; Mannheim, Germany) was used to characterize deposit samples collected from the heat transfer surfaces. Scanning electron microscope imaging was used to identify the morphology of the samples. An X-ray analysis was used for the elemental analysis of the samples.

Cleaning procedure

Two cleaning strategies were evaluated; an acidic wash and a hydraulic wash. Prior to the acidic wash, the concentrate

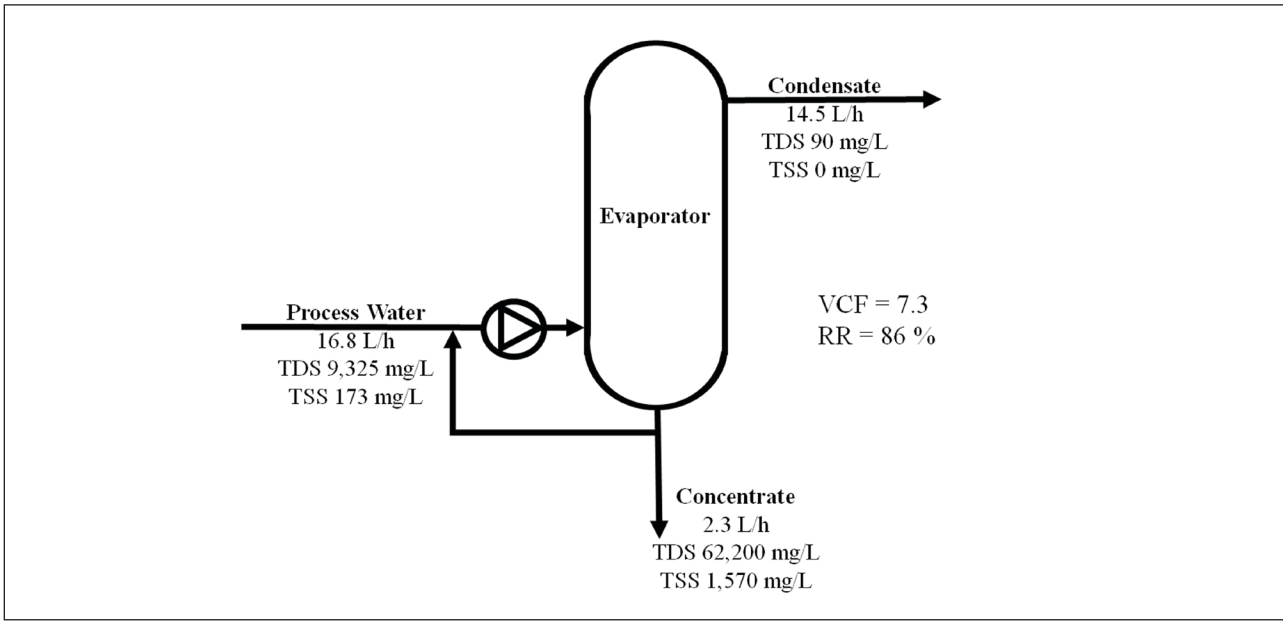

3. Process flow diagram showing average flow rates, total dissolved solids (TDS), and total suspended solids (TSS) concentrations in the evaporator inlet and outlet streams (VFR = volumetric concentration factor; RR = condensate recovery rate).

was drained from the evaporator vessel and the heating surfaces were rinsed by circulating tap water. The deposits on the heating surfaces were then dried to measure their thickness and take samples. For the acidic wash, a targeted pH of 2 was arranged by addition of sulfamic acidic solution. The concentration of the solution was approximately 2.1 g/L, and the wash lasted for 12 h.

After the heating surfaces and remaining deposits were dried again, the hydraulic wash followed. The heating surfaces were sprayed with tap water with a pressure of approximately 3 bar.

Experimental procedure

The pilot plant fouling study was conducted in the following three phases:

Phase I (days 1–35)

In accordance with the maintenance schedule of the paper mill, the pilot plant evaporator was operated continuously for five weeks. The *RR* was set to 86% (*CF* 7). In this time period, the water chemistry of the concentrate was analyzed to evaluate the impact of evaporation on the fouling potential of the concentrated process water. The impact of potential deposit formation on the heating surfaces on the thermal energy balance was evaluated by calculating the *HTC*. At the end of phase I, not enough deposits were formed on the heating surfaces to take samples. Therefore, the trial was continued with increased *RR* in phase II.

Phase II (days 36–50)

To obtain deposits suitable for characterization, the trial was continued for another 15 days with intensified fouling conditions. To promote deposit formation, the *RR* was increased to 90% (*CF* 10). By analyzing where deposits formed, conclusions were drawn as to what caused deposition in the affected areas.

Phase III

After 50 days of continuous operation, the pilot plant evaporator was shut down to take samples for analysis and to evaluate the effectiveness of acidic and hydraulic wash on the removal of deposits from the heating surfaces.

RESULTS AND DISCUSSION

Impact of evaporation on the fouling potential of process water from recycled containerboard mills

The process water of recycled containerboard mills with a restricted water system is characterized by high concentrations of calcium ions. Therefore, the potential for calcium salt fouling is of concern. During evaporation, the concentration of calcium ions is further increased, and the supersaturation concentration of salts present in the water may be exceeded. Based on the mass balance of contaminants in the water, the impact of evaporation on the fouling potential is evaluated. The pilot plant is operated with an evaporation rate of 14.5 L/h and a concentrate discharge volume of 2.3 L/h. This leads to a *VCF* of 7.3 and a resulting *RR* of 86%, as illustrated in **Fig. 3**.

Substances in the process water fed to the evaporator with a boiling point significantly higher than water are expected to be concentrated and are eventually discharged from the evaporator with the concentrate. Substances with a boiling point similar to or lower than water are expected to evaporate. As the process water is characterized by relatively high concentrations of VFAs that potentially contribute to the solubility of calcium carbon-

	Unit	Feed Water	Condensate	Concentrate	Removal Efficiency	Concentrating Factor
pH	-	5.8	3.5	6.0	-	-
TS (TDS +TSS)	mg/L	9,498	-	63,770	-	6.7
TSS	mg/L	173	0	1,570	100%	9.1
TDS	mg/L	9,325	-	62,200	-	6.9
$TDS_{organic}$	mg/L	5,775	-	35,400	-	6.1
$TDS_{inorganic}$	mg/L	3,550	-	26,800	-	7.5
Ca^{2+}	mg/L	903	-	6,900	-	7.3
VFAs*	mg/L	2,766	408	15,757	85.2%	5.7
SO_4	mg/L	475**				

* Sum of acetic, propionic, and n-butyric acids.
**Average of 18 samples taken prior to the trial.
TS = total solids; TSS = total suspended solids; TDS = total dissolved solids; Ca^{2+} = calcium ion; VFAs = volatile fatty acids; COD = chemical oxygen demand, SO_4 = sulfate; TOC = total organic carbon.

II. Concentrations of selected contaminants in the partial streams of the evaporator, removal efficiencies, and concentrating factors.

ate, the entrainment of VFAs in the vapor and the impact on the fouling potential were particularly of interest. Using the terminology of wastewater treatment, the relationship between the concentrations of a contaminant in the condensate to the process water is expressed as the removal efficiency. **Table II** shows the concentration of various contaminants in the process water, condensate, and concentrate, as well as their corresponding concentrating factors (Eq. 5) and removal efficiencies (Eq. 6). The data presented is based on the averages from regular measurements during the period of the trial.

The total solids (TS), which represents the sum of all organic and inorganic constituents, suspended as well as dissolved, in the process water were concentrated from 9,498 to 63,770 mg/L. This is a *CF* of 6.7, which is 8.2% less than the *VCF* of 7.3. As there is no carry-over of suspended solids to the condensate, the difference is entirely due to volatile substances. The *CF* of the organic fraction of TDS is 6.1, a discrepancy of 17% compared with the *VCF*. This is in good agreement with the 14.8% of VFAs that are carried over into the vapor phase. Therefore, it can be assumed the deviation in *CF* for these species and *VCF* overall is primarily due to the entrainment of VFAs in the vapor phase (condensate), where on average 408 mg/L are obtained. This carryover of VFAs also explains the increase in pH of the concentrate to 6.0 compared with the feed pH of 5.8, as well as the low pH of 3.5 of the condensate. It should be noted that the discrepancy is not due to density change. The density of an acetic acid solution with a concentration of 1 wt% is 0.9996 g/cm³ compared to 1.0052 g/cm³ of a solution with a concentration of 5 wt%. The concentrations of the analyzed samples vary between 0.0408% and 1.5767%. As a consequence, differences in density were neglected in this investigation, and the density was assumed to be 1 g/cm³ for all samples.

The concentration of calcium ions in the concentrate was 6,900 mg/L on average. The pH was 6, and the evaporation temperature was 55°C. Therefore, the fouling potential increased compared to the process water. According to experimental data from literature, these conditions could lead to precipitation of calcium carbonate and surface fouling in the evaporator [54]. Due to the elevated temperatures, supersaturation is primarily expected to occur on the heat transfer surfaces. Based on the atomic proportion, 6,900 mg/L of calcium ions would form up to 17,250 mg/L of calcium carbonate. Therefore, theoretically, in 35 days of operation, up to 243 kg of calcium carbonate could precipitate or deposit as foulant on the surfaces of the evaporator. The density of calcium carbonate is 2.71 g/cm³. If buildups were not stopped due to the thermal resistance, this would be a theoretical thickness of 8.6 cm on each of the heating surfaces, assuming even coverage of the lamella surfaces. This theoretical calculation is to demonstrate the potential highly adverse and noticeable effect on the thermal energy balance that this concentration of calcium ions could have. However, as the concentration factor of calcium ions does not differ from the *VCF*, quantitative precipitation of calcium salts did not occur. Also, the daily visual inspections did not show noticeable ongoing deposition on the heating surfaces. Nonetheless, as thermal transmittance could also be impacted by very minor quantities of deposits, the *HTC* was monitored and is reported in the next section.

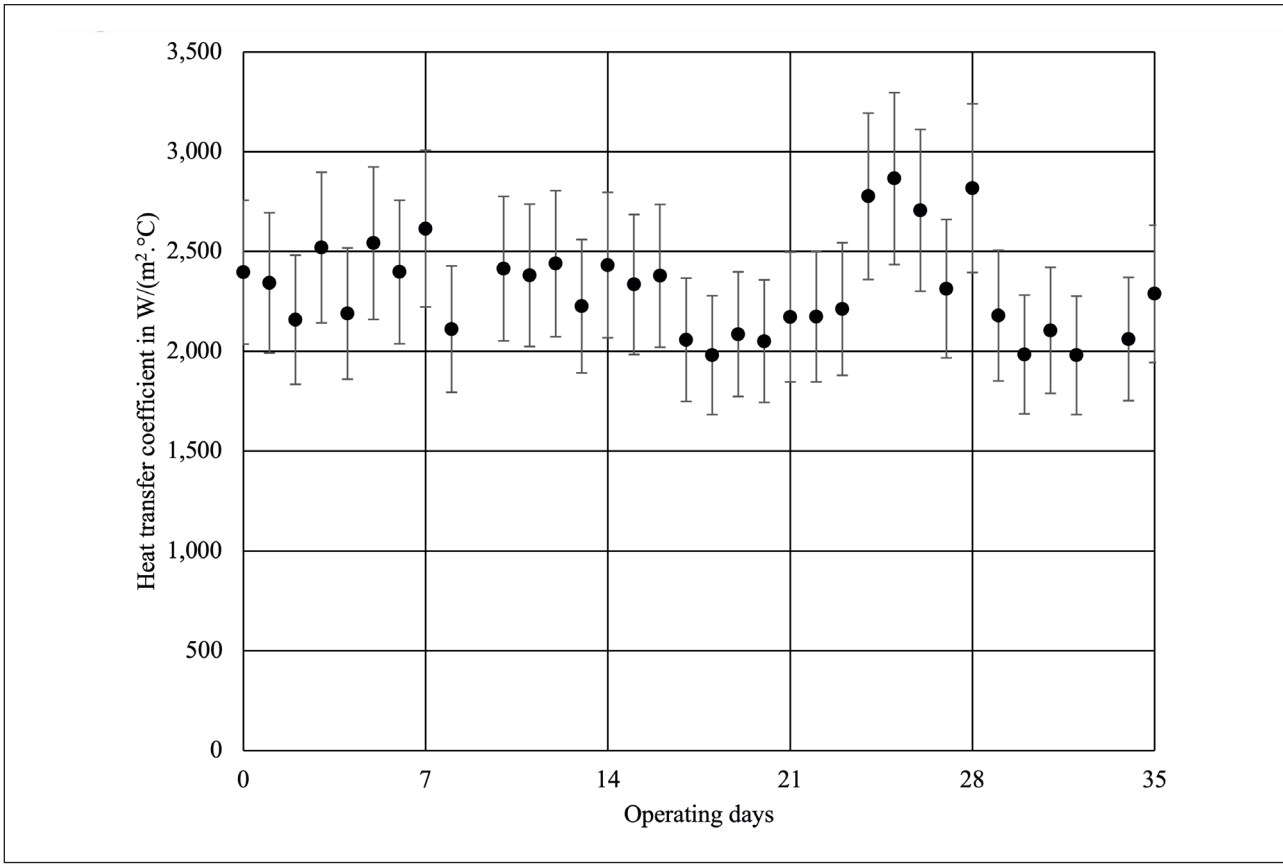

4. Daily heat transfer coefficient over the first 35 days of evaporator operation (error bars: ± 15%).

Monitoring heat transfer coefficient

Also, when the concentration of calcium ions is high, the mass balance does not suggest ongoing fouling. However, due to the low thermal transmittance of calcium salt deposits, minor quantities should already affect the thermal energy balance. Therefore, the *HTC* was monitored.

Evaporation is an energy intensive water treatment method, and maintaining energy efficiency is critical for a viable operation. The economic feasibility of evaporation for the internal purification of process water in recycled containerboard mills heavily depends on whether deposit formation on the heating surfaces impacts the thermal energy balance. Due to the high calcium ion concentration in the process water, the potential for surface fouling is presumably high. The *HTC* of the evaporator pilot plant was monitored over a period of 35 days. This is the maximum time between two maintenance shutdowns at the specific paper mill where the pilot plant is located. The data points are presented in **Fig. 4**.

The *HTC* (Eq. 7) was calculated every day except day 9 and day 33. As can be observed in Fig. 4, the *HTC* was subject to fluctuations. Due to the small dimensions of the plant, the process is sensitive to temperature changes, of which there are several sources. The *HTC* fluctuations relate to variations in ambient and process water temperatures. The pilot plant is located in a well-ventilated chiller room. During working hours, the ambient temperature ranged between 16°C and 32°C. The process water temperature ranged between 20°C and 42°C, depending on the temperature of the process water at the time of sampling, the chiller room ambient temperature, and the water storage time. The pilot plant is only partly insulated to avoid overheating. A temperature change of 0.7°C of one of the temperatures used for calculating heat transfer coefficient results in a change of up to 350 W/(m².C), which corresponds to a 15% deviation from the initial *HTC* of 2,400 W/(m².C). The error bars shown in Fig. 4 indicate this fluctuation range.

Deposits on the heat transfer surfaces would increase thermal resistance and cause a reduction in *HTC* over time. However, an overall downward trend of *HTC* over the time of 35 days was not observed. This means that there is no measurable adverse effect on heat transfer in the evaporator due to deposit formation on the heating bodies within the usual maintenance schedule of the paper mill. The daily visual inspections also confirmed that there was no general deposit formation on the heating surfaces. Only moderate deposits were found at the edges of the heating bodies where the falling film did not sufficiently cover the surfaces. This provided the chance to investigate what constituents in the process water potentially form deposits. As the formed deposits were not pronounced enough to take samples, the trial was continued for another 15 days. To

Parameter	Unit	Average (days 1 to 50)	Average (days 1 to 35)	Average (days 36 to 50)	Maximum Concentration
pH	-	6.03	5.96	6.10	6.5
TS	mg/L	68,156	63,770	75,467	113,400
TSS	mg/L	2,031	1,570	2,800	3,400
TDS	mg/L	66,125	62,200	72,667	110,000
$TDS_{organic}$	mg/L	38,125	35,400	42,667	67,000
$TDS_{inorganic}$	mg/L	28,000	26,800	30,000	43,000
Ca^{2+}	mg/L	7,171	6,900	7,533	11,000
VFAs*	mg/L	16,579	15,757	20,276	25,199

* Sum of acetic, propionic, and n-butyric acids.
TS = total solids; TSS = total suspended solids; TDS = total dissolved solids; Ca^{2+} = calcium ion; VFAs = volatile fatty acids.

III. Concentrate parameters in the different phases of the trial.

promote deposit formation, the recovery rate was increased to 90%. As the changed concentration of the process water impacts the thermal energy balance, *HTC* was no longer monitored in this phase of the trial.

Localized deposit formation

The mass balance of calcium ions and the thermal energy balance both suggest that there is no significant general calcium salt precipitation. Visual inspections suggested localized fouling in areas on the heat transfer surfaces where wetting by the process water flow was insufficient. After 35 days of operation, the deposits were not pronounced enough to take samples. Therefore, the trial was continued for another 15 days. To promote deposit formation, the concentrate discharge volume was reduced from 2.3 to 0.33 L/h to increase the corresponding *RR* from 86% to 90%, and consequently, to raise the calcium ion concentration. **Table III** gives the average values for key process parameters for day 1 to 50, day 1 to 35, day 35 to 50, and the maximum concentrations measured throughout the 50-day trial.

The average calcium ion concentration throughout the trial was 7,171 mg/L, with a maximum of 11,000 mg/L (day 48). The pH was around 6. The high calcium ion concentration at near neutral pH could lead to supersaturation of calcium salts. After 50 days of continuous operation, the deposits on the grit 320 (*Ra* 0.3 µm) and mirror finish (Ra 0.2 µm) heat transfer surfaces were evaluated. The deposits after 50 days of operation can be seen in **Fig. 5**.

As Fig. 5 illustrates, the distribution of deposits on the heating surfaces is non-uniform. Moreover, it can be seen that the patterns of fouling on the two heating bodies are very similar. The thickness of the deposits was comparable on both surfaces. Deposit formation occurred regardless of the surface finish. It even appears that there is a larger area affected on the mirror finish compared to the rougher grit 320 surface. Three regions with pronounced deposit formation were identified and marked in Fig. 5. Deposits formed predominantly from the top right of the surfaces (a), down to the bottom right (b), as well as on the bottom left (c).

Deposit formation occurred where dry patches formed due to insufficient wetting of the surfaces. Dry patches present an opportunity for the formation of a nucleus, as a smaller volume of process water covering the same area on the heat transfer surface will result in more rapid evaporation, higher salt concentrations, and potentially supersaturation, which therefore results in greater fouling.

The upper part of both heating surfaces, especially the upper left quarter, is virtually free of any deposits. Here, the falling film was stable and the surfaces were well covered. In contrast, the lower right sides of the surfaces show fouling with a thickness of more than 2 mm. The reason is that the falling film does not entirely cover the right edges of the surfaces, and deposits form and further adversely affect liquid flow, causing the deposits to grow and spread. This explains why it appears that deposition increases from top to bottom of the surfaces. Formed deposits redirect the falling film and lead to a channeling effect. This can be seen at the bottom middle where the relative higher flow rate due to redirected flow from deposits on the sides prevented fouling. Deposits also formed on the bottom left of both surfaces with a thickness of up to 1.4 mm. The reason again is dry patches; here, these are due to shrinkage of the falling film.

Wetted surfaces such as the top left or the bottom middle were well covered and salts did not reach their supersaturation concentration, so therefore no fouling occurred. The uniform distribution of the liquid and formation of a stable falling film are crucial, as film thickness prevents supersaturation of dissolved salts and flow velocity creates a dragging force that washes off particles.

The insufficient coverage of the heating surfaces allowed investigation of fouling of the process water that generally

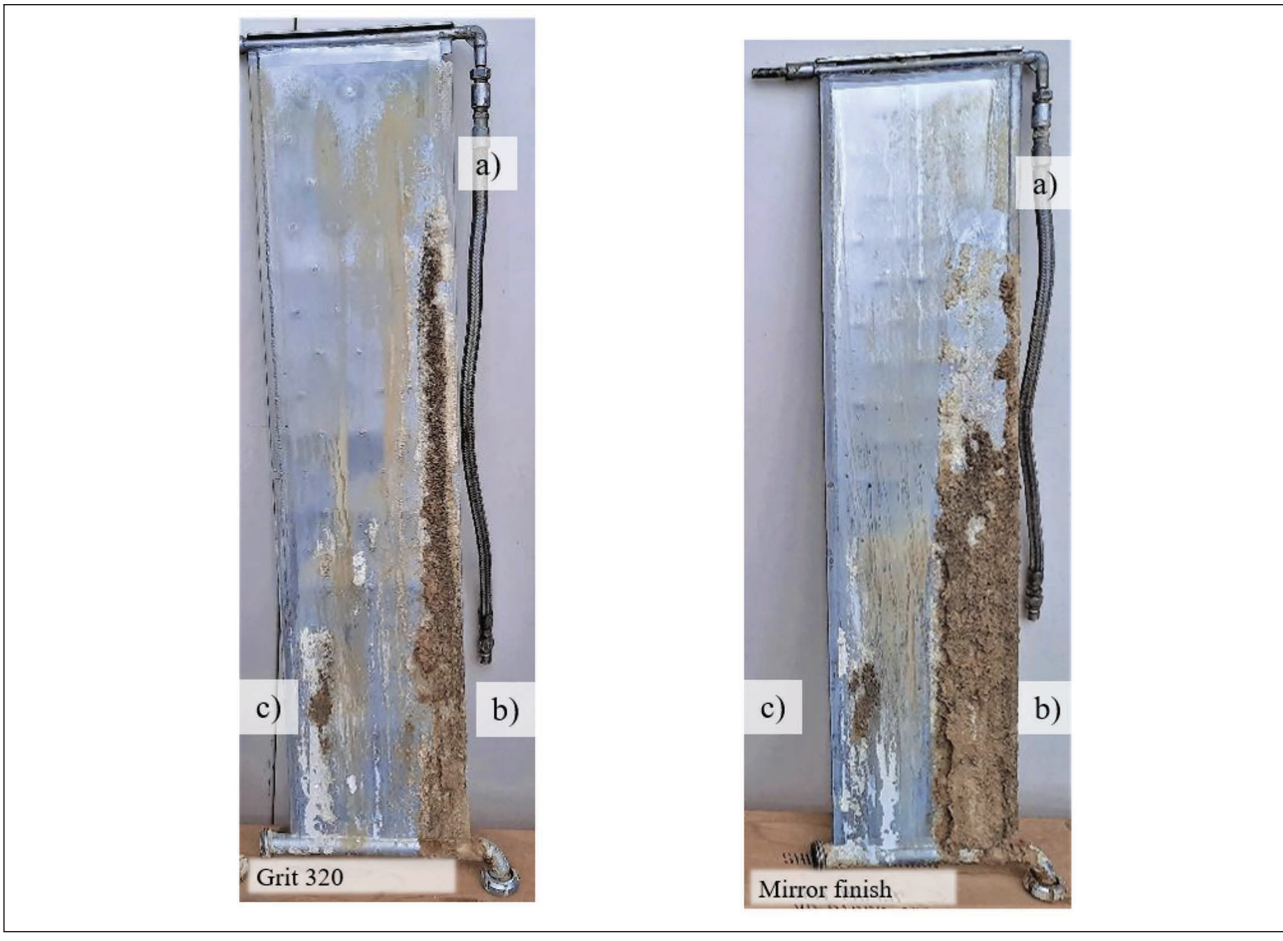

5. Deposits formed on the evaporator heating surfaces after 50 days of continuous operation.

does not form deposits under the investigated conditions. The following characterization of deposits helped to identify the constituents in water that potentially cause fouling. Moreover, it was possible to investigate cleaning strategies.

Deposit characterization

Deposit samples were taken from the three identified locations affected by fouling (Fig. 5). Only samples directly in contact with the heating surfaces were characterized to assure identification of the constituents that initiate deposit formation. The following characterization of the samples covers determination of organic as well as inorganic fraction, morphology, and elemental analysis.

Organic and inorganic fractions

Representative deposit chips were scraped off the heating surfaces. First, samples were dried in an oven at 105°C. Then, the loss on ignition was determined in a furnace at 550°C. The weight difference provides information about volatile organic and incombustible inorganic material. The results are shown in **Table IV**.

The analysis revealed that the composition of deposits is consistent across the sampled areas of the heat transfer surface and consists, on average, of 85% inorganic and 15% organic material.

Sample	Dried Sample, g	Incombustible, g	Organic Fraction, %	Inorganic Fraction, %
1	11.449	9.500	17.0	83.0
2	8.692	7.312	15.9	84.1
3	7.683	6.669	13.2	86.8
4	3.627	3.132	13.6	86.4

IV. Organic and inorganic fractions of deposit samples.

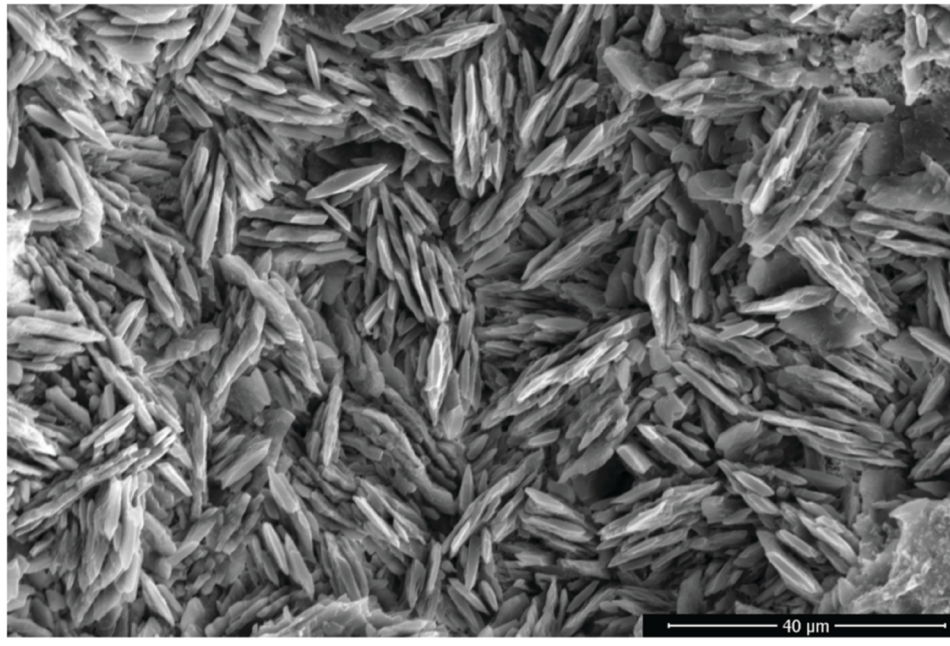

6. Exemplary scanning electron microscope (SEM) image of scale deposited on the heating surfaces of the evaporator pilot plant after 50 days of operation.

Morphology

Scanning electron microscope imaging provides information about the morphology of the samples. The SEM image in **Fig. 6** shows the characteristic crystalline structure of the deposits at a magnification of 3,000.

The morphology depicted in Fig. 6 shows flattened, elongated, needle-like crystals. Clusters of sharp, bladed plates in parallel arrangements form desert rose-like structures. This could suggest selenite, a form of gypsum that is the dihydrate polymorph of calcium sulfate ($CaSO_4 \cdot 2\,H_2O$).

Elemental analysis

The individual elements present in the samples were identified by energy-dispersive X-ray analysis (EDX). **Figure 7** shows peaks for the elements oxygen, sulfur, and calcium.

The dominance of oxygen, sulfur, and calcium confirms the assumption from SEM imaging. Therefore, deposits on the heating surfaces are calcium sulfate. The calcium can be traced back to the calcium carbonate that is contained in graphical paper grades that enter the paper recycling process with the recovered paper, and the sulfate stems from kraft-containing packaging paper grades (pulp produced with the sulfate process). As $CaSO_4$ is not sensitive to pH, a wash using EDTA might be more effective compared to the sulfamic acid that was used.

Effectiveness of acidic and hydraulic washes

The prior sections demonstrated that the water chemistry of recycled containerboard mills with restricted water systems does not cause general fouling. However, deposits were found in areas where the heating surfaces were not covered sufficiently. Therefore, the effectiveness of cleaning strategies was investigated.

The thickness of deposits was measured after two cleaning steps in order to evaluate their effectiveness. Based on the identified areas affected by fouling that are marked in Fig. 5, the thickness of representative deposit samples was measured. When the thickness of deposits varied, a range is presented. The results for the mirror, as well as grit 320 surfaces, before and after acidic and pressure washes are summarized in **Table V**.

The acidic wash reduced the thickness of deposits with a thickness of up to 1.4 mm by up to 1.25 mm (mirror finish, area c). Deposits with a thickness of 2 mm were reduced by up to 1.1 mm (mirror, area b). The low-pressure wash reduced the thickness of deposits with a thickness of 2 mm by up to 1.90 (mirror, b). The thickness of deposits after acidic and hydraulic wash appears to be less on the mirror finish compared to the grit 320. This may confirm less persistent deposits and easier cleaning on smoother surfaces.

Before each wash, the deposits were dried to determine their thickness. Therefore, it needs to be considered that the samples had to be rewet for each cleaning step. Furthermore, it is worth mentioning that deposits formed in areas because the surface coverage was not sufficient. Therefore, the surface coverage during the acidic wash was also reduced and similar channeling effects of the flow, as well as film shrinkage, were also applied to the washing process. This impacts the cleaning result.

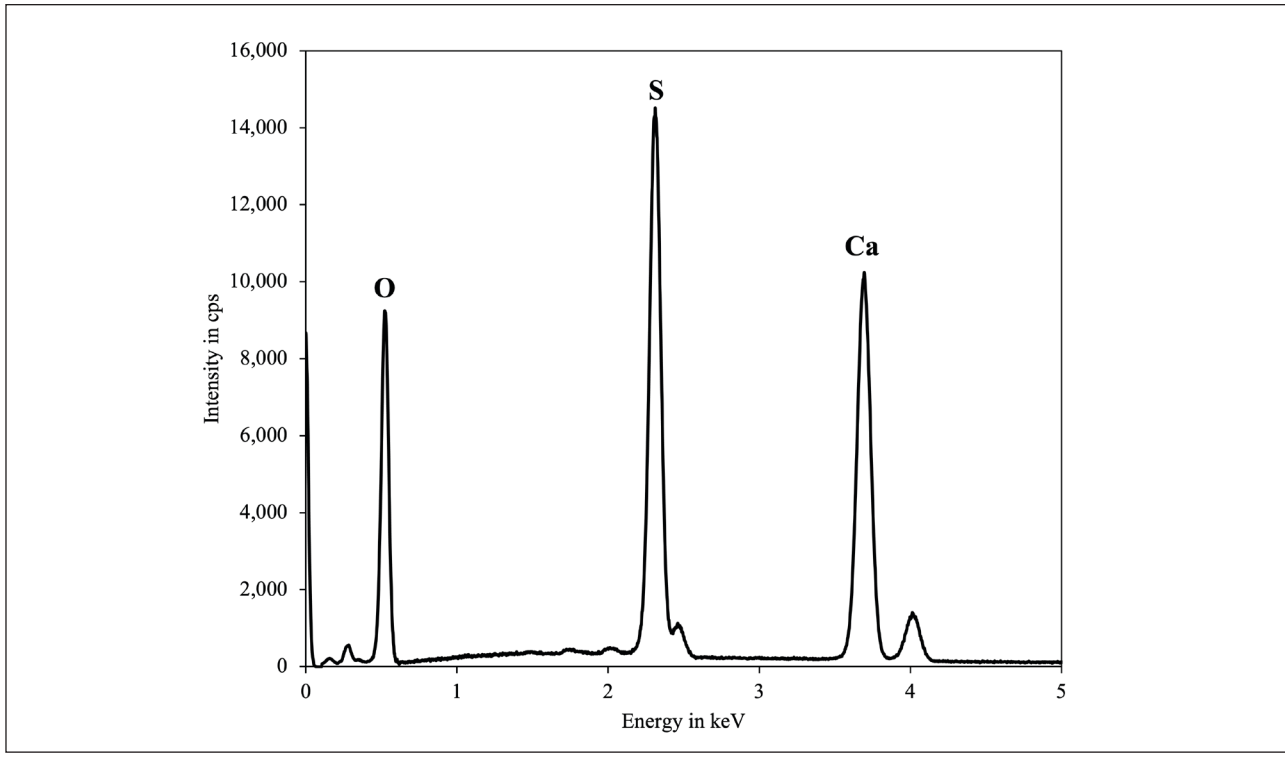

7. Results of scanning electron microscope-energy-dispersive X-ray analysis (SEM-EDX) analysis of the deposit presented in Fig. 6.

	Mirror Finish			Grit 320		
Area*	After 50 Days	After Acidic Wash	After Low Pressure Wash	After 50 Days	After Acidic Wash	After Low Pressure Wash
a)	0.70	0.10	0.10	0.70	0.40	0.10
b)	> 2.00	0.90–2.00	0.10–0.75	> 2.00	1.40–2.00	0.90–2.00
c)	1.40	0.15	0.05	1.35	0.15	0.15
* As defined in Fig. 5.						

V. Impact of acid and hydraulic washes on the deposit thicknesses (mm) on mirror finish and grit 320 heating surfaces.

CONCLUSIONS

The fouling behavior of process water from a recycled containerboard mill in a vacuum evaporator pilot plant was studied.

After 35 days of continuous operation, the heat transfer coefficient was not noticeably reduced by foulant deposition. After 15 more days of operation with increased concentration factor, there were still large areas of the heat transfer surfaces without deposits. Fouling therefore did not impact the energy efficiency within the usual maintenance interval of a paper mill (35 days) and there was no general fouling due to the specific water chemistry of recycled containerboard mills despite the high calcium ion concentration.

Deposits were only found locally in areas where the heating surfaces were not sufficiently covered by process water. For a potential scale up, this shows that the stability and hydrodynamics of the falling film and surface wetting are critical to avoid deposit formation. Buildups on the mirror finish and grit 320 surfaces showed a similar pattern as well as similar thickness, leading to the conclusion that there is no significant advantage of designing a full scale evaporator with a more expensive mirror finish compared to grit 320 in regards to deposit formation.

Deposits with a thickness of up to 1.4 mm were removed with a sulfamic acid wash. The deposits after cleaning appear to be slightly thicker on the grit 320 surface; thus, it may be concluded that the mirror finish is easier to clean compared to the grit 320 surface. The main constituents in the deposits suggest calcium sulfate as foulant. Therefore, cleaning with EDTA might be more effective than sulfamic acid.

The overall conclusion from this pilot plant study is that the use of evaporators for recovering water in recycled containerboard mills is not limited by fouling, either from an operational or an energy efficiency perspective. Evaporator technology therefore presents a useful option for complete water system closure in recycled containerboard mills where conditions justify the investment and operational cost. **TJ**

ACKNOWLEDGEMENTS

The authors would like to acknowledge Visy Industries for providing the pilot plant, process water, support, and technical assistance. Project support was provided by the Australian Research Council ITRH Processing Advanced Lignocellulosics (IH170100020). The authors acknowledge the use of the instruments and scientific and technical assistance of Dr. Xi-Ya Fang at the Monash Centre for Electron Microscopy, a Node of Microscopy Australia.

LITERATURE CITED

1. Verband Deutscher Papierfabriken e.V., "Paper 2020 annual report," Bonn, 2020, p. 77.
2. Valeeva, N. and Li, X., "Flipping the world: Challenges of growing North America recycled containerboard," RaboResearch Food & Agribusiness, Utrecht, Netherlands, 2017. Available [Online] https://research.rabobank.com/far/en/sectors/fa-supply-chains/flipping-the-world-challenges-of-growing-north-america-recycled-containerboard.html <10July2023>.
3. Suhr, M., Klein, G., Kourti, I., et al., "Best available techniques (BAT) reference document for the production of pulp, paper and board," JRC Science and Policy Reports, European Commission, Seville, Spain, 2015, p. 575.
4. Berg, P. and Lingqvist, O., "Pulp, paper, and packaging in the next decade: Transformational change," McKinsey, Stockholm, May 2017.
5. Mekonnen, M.M. and Hoekstra, A.Y., *Sci. Adv.* 2(2): e1500323(2016). https://doi.org/10.1126/sciadv.1500323.
6. Tong, T. and Elimelech, M., *Environ. Sci. Technol.* 50(13): 6846(2016). https://doi.org/10.1021/acs.est.6b01000.
7. Jung, H. and Kappen, J., *Prof. Papermaking* 11(2): 11(2014).
8. Bienert, C. and Persin, C., *Wochenbl. Papierfabr.* 146(3): 158(2018).
9. Miranda, R., Blanco, A., and Negro, C., *Chem. Eng. J.* 148(2): 385(2009). https://doi.org/10.1016/j.cej.2008.09.014.
10. Auhorn, W.J., "Chemical additives," in *Handbook of Paper and Board* (H. Holik, Ed.), John Wiley & Sons, Weinheim, 2006. https://doi.org/10.1002/3527608257.ch3.
11. Laufmann, M., "Pigments as fillers," in *Handbook of Paper and Board* (H. Holik, Ed.), John Wiley & Sons, Weinheim, 2006, pp. 33-54.
12. Borchers, B. and Heider, U., "Erfassung und Charakterisierung der bei der Herstellung graphischer Recyclingpapiere mit dem Altpapierstoff eingetragenen Stärke," PTS Research Report, Papiertechnische Stiftung, Heidenau, Germany, 2006.
13. Habets, L., *Pulp Pap. Int.* 45(12): 26(2003).
14. Hamm, U. and Schabel, S., *Water Sci. Technol.* 55(6): 205(2007). https://doi.org/10.2166/wst.2007.230.
15. Berard, P., *Pulp Pap. Int.* 42(4): 44(2000).
16. Bürgmayr, S., Tanner, J., Batchelor, W., et al., *Nord. Pulp Pap. Res. J.* 38(1): 181(2023). https://doi.org/10.1515/npprj-2022-0042.
17. Meyer, T. and Edwards, E., *Water Res.* 65: 321(2014). https://doi.org/10.1016/j.watres.2014.07.022.
18. McCarty, P.L., *Public Works* 95(9): 107(1964).
19. Hamm, U., Bobek, B., Demel, I., et al., *Das Papier* 1: 46(2001).
20. Schabel, S., Putz, H.J., Hamm, U., et al., *TAPPI J.* 13(11): 47(2014) https://doi.org/10.32964/TJ13.11.47.
21. Batstone, D.J., Landelli, J., Saunders, A., et al., *Water Sci. Technol.* 45(10): 187(2002). https://doi.org/10.2166/wst.2002.0326.
22. Mänttäri, M., Kallioinen, M., and Nyström, M., "Membrane technologies for water treatment and reuse in the pulp and paper industries," in *Advances in Membrane Technologies for Water Treatment* (A. Basile, A. Cassano, and N.K. Rastovi, Eds.), Woodhead Publishing, Sawston, UK, 2015, pp. 581-603. https://doi.org/10.1016/B978-1-78242-121-4.00019-8.
23. Cainglet, H.E., Saavedra, T., Bürgmayr, S., et al., *J. Water Process. Eng.* 44: 102407(2021). https://doi.org/10.1016/j.jwpe.2021.102407.
24. Richardson, D., Blom, L., and Reeves, E., "Pilot plant investigations into the feasibility of membrane treatment of paper machine and deinking plant filtrates," *Appita Annu. Conf., 62nd*, Appita, Macleod, VIC, Australia, 2008, p. 383.
25. Wirth, B., Kosse, J., and Welt, T., *Wochenbl. Papierfabr.* 133(16): 974(2005).
26. Huuha, T.S., Kurniawan, T.A., and Sillanpää, M., *Chem. Eng. J.* 158(3): 584(2010). https://doi.org/10.1016/j.cej.2010.01.058.
27. Güneysu, S. and Aydın, S., *Desalin. Water Treat.* 93: 195(2017). https://doi.org/10.5004/dwt.2017.21012.
28. Gullichsen, J., Paulapuro, H., and Fogelholm, C.-J., *Chemical Pulping*, Papermaking Science and Technology Series, Book 6, Fapet Oy, Helsinki, 2000, pp. 41-42.
29. Bajpai, P., "Basic overview of pulp and paper manufacturing," in *Green Chemistry and Sustainability in Pulp and Paper Industry*, Springer International Publishing, Cham, 2015, pp. 11-39. https://doi.org/10.1007/978-3-319-18744-0.
30. Ward, R.O., Manolescu, D.R., and Sweet, F.W., "Millar Western Meadow Lake. A success story in effluent treatment," *Joint Conference of Environment Canada and the German Ministry of Environment*, Environment Canada/Germany Ministry of Environment, Gatineau, QC, Canada/Bonn, Germany, 1993.
31. Young, J., *Pulp Pap.* 68(3): 73(1994).
32. Fosberg, T., Lloyd, L., and Kelland, C., "Case study: CRMP effluent recycling system at the Australian forest industries Myrtleford mill," *Appita Annu. Conf., 47th*, Appita, Macleod, VIC, Australia 1993.
33. NCASI, "Pulp mill process closure: A review of global technology developments and mill experiences in the 1990s," Technical Bulletin No. 860, National Council for Air and Stream Improvement, Cary, NC, USA, 2003, p. 44-56.
34. Fosberg, T. and Sweet, B., *Environmental Progr.* 13(3): 163(1994). https://doi.org/10.1002/ep.670130310.
35. Koistinen, P.R, *AWT98*, International Water Assn., London, 1998, p. 623.
36. Bentley, D.J., Jr., *TAPPI J.* 82(1): 59(1999).

37. Rodden, G., *Pulp Pap. Int.* 54(4): 23(2012).
38. Xu, J., Xie, J., Cheng, Z., et al., *J. Environ. Manage.* 292: 112740(2021). https://doi.org/10.1016/j.jenvman.2021.112740.
39. Gallerani, P.A., Brown, D., and Moore, G., "Evaluation of the Hadwaco MVR Evaporator for the metal finishing industry," U.S. Environmental Protection Agency, Washington, DC, 2001.
40. Burkhart, H., Koistenen, P., Kothe, K.D., et al., *Ipw* 4: 41(2002).
41. Ramm-Schmidt, L., "New low cost evaporation process for recovery of dissolved solids in very dilute process streams," *Separation Processes in the Sugar Industry — Proceedings of SPRI Workshop*, Sugar Processing Research Institute Inc., New Orleans, LA, USA, 1996.
42. Taborek, J., *Chem. Eng. Prog.* 68(2): 59(1972).
43. Steinhagen, R., Müller-Steinhagen, H., and Maani, K., *Heat Transfer Eng.* 14(1): 19(1993). https://doi.org/10.1080/01457639308939791.
44. Müller-Steinhagen, H., Malayeri, M.R., and Watkinson, A.P., *Heat Transfer Eng.* 30(10-11): 773(2009). https://doi.org/10.1080/01457630902744119.
45. Garrett-Price, B., "Characteristics, costs, prevention, control and removal," in *Fouling of Heat Exchangers*, Noyes Publications, Park Ridge, NJ, USA, 1985, p. 417.
46. Thackery, P.A., *Effluent Water Treat. J.* 20(3): 111(1980).
47. Pritchard, A., "The economics of fouling," in *Fouling Science and Technology*, Springer Dordrecht, Dordrecht, Netherlands, 1988, pp. 31-45. https://doi.org/10.1007/978-94-009-2813-8_3.

ABOUT THIS PAPER

Cite this article as:
Bürgmayr, S., Tanner, J., Batchelor, W., et al., *TAPPI J.* 22(7): 474(2023). https://doi.org/10.32964/TJ22.7.474

DOI: https://doi.org/10.32964/TJ22.7.474

ISSN: 0734-1415

Publisher: TAPPI Press

48. Müller-Steinhagen, H., "Fouling of heat exchanger surfaces," in *VDI Heat Atlas*, VDI Verlag, Düsseldorf, 1993, pp. 79-104. https://doi.org/10.1007/978-3-540-77877-6_7.
49. Bott, T.R., *Exp. Therm. Fluid Sci.* 14(4): 356(1997). https://doi.org/10.1016/S0894-1777(96)00137-9.
50. Kern, D.Q. and Seaton, R.A., *Br. Chem. Eng.* 4(5): 258(1959).
51. Zhao, X. and Chen, X.D., *Heat Transfer Eng.* 34(8-9): 719(2013). https://doi.org/10.1080/01457632.2012.739482.
52. Sheikholeslami, R., *AIChE J.* 49(1): 194(2003). https://doi.org/10.1002/aic.690490117.

ABOUT THE AUTHORS

Bürgmayr

Tanner

Batchelor

Hoadley

This project was a Ph.D. research collaboration between Monash University and Visy Industries to investigate the feasibility of evaporation for water system closure in recycled board mills. This research is the first long-duration on-site pilot plant study investigating fouling phenomena of process water from recycled board mills during evaporation. It complements a prior research project characterizing the process water using a thermodynamic model, as well as a research project on fouling of an ultrafiltration pilot plant.

The most difficult aspect of this study was that the custom-built pilot plant was installed on-site at a paper mill, and prior to the fouling studies, it had to be modified and optimized to guarantee useful and accurate testing results.

We found that calcium-rich process water from paper mills does not necessarily lead to fouling and allows the use of evaporation without loss of heat transfer and overall energy efficiency. Interestingly, state-of-the-art vacuum evaporators with mechanical vapor recompression have a relatively low energy consumption. Compared to anaerobic treatment and membrane filtration, the principle of evaporation appears to be much more suitable to close water systems.

This research provides insights that allow comparison of biological treatment, membrane filtration, and evaporation. If evaporation is considered for a mill, this study gives insights in regards to operation, selectivity, and overall energy efficiency. The next step is that Visy Industries will conduct an economic feasibility study and consider the use of evaporators at all recycled board mills in Australia.

Bürgmayr is a former Ph.D. student, Tanner is lecturer, Batchelor is associate professor, and Hoadley is associate professor in the Department of Chemical and Biological Engineering at Monash University in Clayton, VIC, Australia. Email Hoadley at andrew.hoadley@monash.edu.

53. Tianqing, L., Yuwen, S., and Wang, X., "Formation and removal processes of calcium carbonate fouling," *Mitigation and Heat Exchanger Fouling Conf.*, Begell House, Danbury, CT, USA, 1999.
54. Coto, B., Martos, C., Pena, J.L., et al., *Fluid Phase Equilib.* 324: 1(2012). https://doi.org/10.1016/j.fluid.2012.03.020.
55. Geddert, T., Bialuch, I., Augustin, W., et al., *Heat Transfer Eng.* 30(10-11): 868(2009). https://doi.org/10.1080/01457630902753789.
56. Kazi, S., Duffy, G., and Chen, *X., Appl. Therm. Eng.* 30(14-15): 2236(2010). https://doi.org/10.1016/j.applthermaleng.2010.06.005.
57. Rankin, B. and Adamson, W., *Desalination* 13(1): 63(1973). https://doi.org/10.1016/S0011-9164(00)80092-2.
58. Lei, C., Peng, Z., Day, T., et al., *Heat Mass Transfer* 38(1): 25(2011). https://doi.org/10.1016/j.icheatmasstransfer.2010.10.006.
59. Stärk, A., Krömer, K., Loisel, K., et al., *Heat Transfer Eng.* 38(7-8): 762(2017). https://doi.org/10.1080/01457632.2016.1206418.
60. Mwaba, M., Rindt, C.C.M., Van Steenhoven, A.A., et al., *Heat Transfer Eng.* 27(3): 42(2006). https://doi.org/10.1080/01457630500458187.
61. Pääkkönen, T.M., Riihimäki, M., Puhakka, E., et al., "Crystallization fouling of $CaCO_3$ — effect of bulk precipitation on mass deposition on the heat transfer surface," *Conf. on Heat Exchanger Fouling and Cleaning*, Heat Transfer Research Inc., Navasota, TX, USA, 2009.
62. Teng, K.H., Kazi, S.N., Amiri, A., et al., *Powder Technol.* 315: 216(2017). https://doi.org/10.1016/j.powtec.2017.03.057.
63. Baier, R.E., Meyer, A.E., DePalma, V.A., et al., *J. Heat Transfer* 105(3): 618(1983). https://doi.org/10.1115/1.3245630.
64. Visser, J., "Adhesion and removal of particles I," in *Fouling Science and Technology*, Springer, Dordrecht, 1988, pp. 87-104. https://doi.org/10.1007/978-94-009-2813-8_7.
65. Oliveira, R., *Exp. Therm. Fluid Sci.* 14(4): 316(1997). https://doi.org/10.1016/S0894-1777(96)00134-3.
66. Quan, X., Geng, Y., Yuan, P., et al., *Chem. Eng. Sci.* 135: 52(2015). https://doi.org/10.1016/j.ces.2015.06.055.
67. Schmidl, W., Frederick W.J., "Current trends in evaporator fouling," I*nt. Chem. Recovery Conf.*, TAPPI Press, Atlanta, 1998.
68. Müller-Steinhagen, H. and Branch, C.A., *Exp. Therm. Fluid Sci.* 14(4): 425(1997). https://doi.org/10.1016/S0894-1777(96)00143-4.
69. Li, Y. and Watkinson, A.P., *Heat Transfer Eng.* 32(3-4): 258(2011). https://doi.org/10.1080/01457632.2010.495614.
70. Jamialahmadi, M. and Mueller-Steinhagen, H., *Heat Transfer Eng.* 12(4): 19(1991). https://doi.org/10.1080/01457639108939760.
71. Roebuck, A.H. and Bennett, C.A., *Oil Gas J.* 75(37): 93(1977).
72. Agilent, *Agilent 5975 Series MSD 2012, Operational Manual*, Agilent Technologies, Santa Clara, CA, USA, 2012.